Irreversible properties of superconducting $HoNi_2B_2C$ single crystals

C. Krutzler,[1,*] R. Fuger,[1] M. Eisterer,[1] G. Fuchs,[2] G. Behr,[2] and H. W. Weber[1]
[1]*Atomic Institute of the Austrian Universities, 1020 Vienna, Austria*
[2]*Institut für Festkörper- und Werkstofforschung Dresden, 14109 Dresden, Germany*
(Received 21 April 2005; revised manuscript received 16 August 2005; published 11 October 2005)

We report on magnetic measurements on a $HoNi_2B_2C$ single crystal. The magnetic and the superconducting phase diagrams were determined in different crystal directions and the superconductive properties evaluated as a function of temperature and applied field. The results on the critical current densities reveal bulk pinning in those regions of the phase diagram, where superconductivity is not suppressed by metamagnetically ordered structures of the Ho $4f$ moments.

DOI: 10.1103/PhysRevB.72.144508 PACS number(s): 74.70.Dd, 74.25.Sv, 74.25.Dw, 74.25.Ha

I. INTRODUCTION

The members of the superconducting borocarbide family RNi_2B_2C, where R is a rare-earth element, attracted a lot of interest mainly for two reasons: First, the related compound YPd_2B_2C with a T_c of about 23 K (Ref. 1) showed the highest known transition temperature of bulk intermetallics at the time of it's discovery. Furthermore, some sort of systematic investigation of T_c was possible by either substituting the rare-earth element or the transition metal in this class of superconductors. Second, the interplay between superconductivity and magnetism that appears for the rare-earth elements Ho, Er, Tm, and Dy, can be studied readily, because T_c and the temperature for the magnetic transition T_N are of the same order. (For a review see Ref. 2.)

$HoNi_2B_2C$ belongs to these so called magnetic borocarbide superconductors. It shows a superconducting transition at about 8.5 K and a transition to an antiferromagnetically ordered state at T_N=5.2 K. $HoNi_2B_2C$ is particularly interesting, because other complex magnetic phases, in addition to the antiferromagnetic order, are observed to coexist with superconductivity in certain temperature ranges. The magnetic moments of Ho are oriented in the ab plane and order differently in three temperature regimes. The situation can be summarized as follows. At zero field and temperatures below 5.2 K, the Ho moments are antiferromagnetically ordered (transition denoted further on as T_N), whereas for temperatures above ~6 K paramagnetic behavior prevails (transition T_m). The antiferromagnetically ordered state can be visualized as ferromagnetic planes aligned along the [110] directions which are rotated by 180° with respect to each other along the c axis. Additionally, in the temperature range $T_N < T < T_m$, there are two incommensurate antiferromagnetic structures at zero field, namely a spiral structure along the tetragonal c axis with a modulation vector $\tau_2 \approx (0,0,0.916)$ and an a axis modulated structure [modulation vector $\tau_3 \approx (0.58,0,0)$]. Details about the magnetism in $HoNi_2B_2C$ were mainly revealed by neutron diffraction measurements and can be found in Refs. 3–8.

For magnetic fields applied perpendicular to the c axis of $HoNi_2B_2C$ single crystals, up to three metamagnetic transitions have been found from magnetization and elastic neutron diffraction measurements. Besides the paramagnetic phase at elevated temperatures and the simple antiferromagnetic phase ($\uparrow\downarrow\uparrow$) which is observed at low temperatures in zero field and at low applied fields, three additional low-temperature phases were found to occur for sufficiently high fields. These metamagnetic phases can be denoted by the arrow combinations $\uparrow\uparrow\downarrow$, $\uparrow\uparrow\rightarrow$, and $\uparrow\uparrow\uparrow$, as first introduced in Ref. 6. The arrows refer to the orientation of the magnetic moments with respect to the [110] crystal direction, arrow $\uparrow$ indicating nearly parallel moments to [110], arrow $\downarrow$ nearly antiparallel, or arrow $\rightarrow$ nearly perpendicular to [110]. Magnetic phase diagrams in the H-T plane for fields applied along the a axis and the [110] axis were experimentally established,[9,10] where the four magnetic phases ($\uparrow\downarrow\uparrow$, $\uparrow\uparrow\downarrow$, $\uparrow\uparrow\rightarrow$, and $\uparrow\uparrow\uparrow$) are separated from each other by the lines $B_N(T)$, $B^*(T)$, and $B_m(T)$. Furthermore, a strength-of-field, angle-of-field phase diagram at low temperatures was proposed,[6] based on in-plane angular studies. This phase diagram has been derived also from a theoretical model which incorporates crystalline electric field effects to produce a four-position clock model for the isolated moments and the exchange interaction including three nearest neighbors.[11] Another microscopic approach to explain this phase diagram used a one-dimensional model, in which the presence of ferromagnetically ordered Ho layers with their magnetic moments oriented perpendicular to the c axis was assumed from the very beginning and the competition of the Ruderman-Kittel-Kasuya-Yosida (RKKY) interaction along the c axis with the crystalline electric field was analyzed.[12] Interestingly, the metamagnetic phase represented by ($\uparrow\uparrow\rightarrow$) has a modulation vector close to τ_3 of the incommensurate a-axis modulated structure as found by elastic neutron diffraction at 2 K.[7,10] The presence of an a^*-metamagnetic phase at 2 K was also supported by elastic neutron diffraction on $HoNi_2B_2C$ powder.[13] The extension of the low-temperature metamagnetic phases to incommensurate zero-field phases at elevated temperatures was supported by specific heat measurements.[14] In particular, $B^*(T)$ separating the metamagnetic phases ($\uparrow\uparrow\downarrow$) and ($\uparrow\uparrow\rightarrow$) corresponds at zero field to a transition temperature T^*, which is ascribed to a change from a dominant a^* to a dominant c^* phase.[14]

$HoNi_2B_2C$ has a layered crystal structure that leads to an anisotropic behavior of the superconducting and the magnetic properties. It is also known that the superconducting

properties, especially between T_N and T_c, are very sensitive to details of the sample preparation and to small deviations from the ideal stoichiometry (cf. Refs. 15 and 16). Depending on details of the preparation route, reentrant or near-reentrant behavior was observed in $HoNi_2B_2C$. The incommensurate magnetic structures suppressing superconductivity within a narrow temperature range are responsible for the reentrant behavior, whereas the antiferromagnetic state coexists with superconductivity at temperatures below T_N. The issue of which of the two incommensurate structures destroys the superconducting state has been controversially discussed.[16–19]

The flux pinning properties of this material in the superconducting state were so far only investigated to a minor extent. Investigations by small angle neutron scattering (Refs. 20–23) showed the existence of a well-formed vortex lattice over much of the phase diagram indicating the absence of strong pinning effects. Reference 24 examined a possible effect of magnetic ordering on the pinning of vortices. For fields applied parallel to the [001] crystal direction, the vortex lattice in $HoNi_2B_2C$ was found to be weakly pinned and dominated by surface barriers at temperatures below ~5 K and above ~6 K, while in the region, where the incommensurate *a*-axis modulated structure appears, clear evidence for bulk pinning was found. The authors proposed pinning of vortices by this *a*-axis magnetically ordered state as an explanation.

A similar situation was found in $ErNi_2B_2C$. Magnetic ordering into an incommensurate structure, again modulated along the *a* axis, sets in within the superconducting state and leads to bulk pinning for fields parallel to [001].[25,26] Similarly to $HoNi_2B_2C$, a connection between the magnetic structure and bulk pinning was inferred.

The present paper reports on detailed studies of the superconducting, particularly the irreversible, properties of $HoNi_2B_2C$ single crystals and reveals bulk pinning in the entire region of the phase diagram.

II. EXPERIMENT

The $HoNi_2B_2C$ single crystal was prepared by the floating zone technique with optical heating.[27,28] Its dimensions are 0.9×1.36 mm^2 in the *ab* plane and 2.03 mm in the *c* direction. The crystal was investigated by magnetic measurements in a commercial superconducting quantum interference device (SQUID) magnetometer (Quantum Design) in fields of up to 1 T and employing an ac option, as well as in a vector vibrating-sample magnetometer (VSM) (Oxford Instruments) providing fields of up to 5 T and full angular analysis.

The upper critical fields $\mu_0 H_{c2}$ were determined from ac SQUID measurements with an ac field amplitude of 30 μT. A tangent criterion fitting the linear slope of the in-phase signal of the susceptibility $m'(T)$ was used for the evaluation. Some examples of such measurements with the field along the [100] direction are shown in Fig. 1 for different dc fields between 0 and 450 mT. The H_{c2} evaluation is demonstrated for the 100 mT curve. Without dc field reentrant superconductivity does not occur, whereas reentrant behavior is observed whenever a dc field is applied.

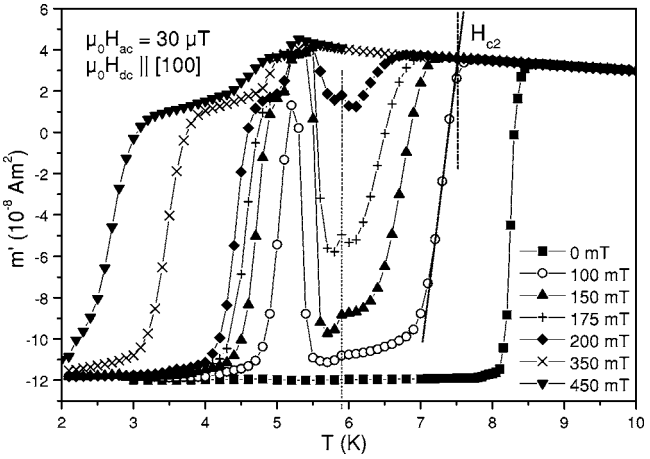

FIG. 1. The ac measurements in the dc fields between 0 and 450 mT applied along the [100] crystal direction. At $\mu_0 H=0$ mT, no reentrant behavior occurs, whereas for fields >0 reentrant superconductivity is observed. The evaluation criterion for H_{c2} is demonstrated for the 100 mT measurement. The vertical dashed-dotted line at 5.9 K indicates the magnetic transition T_m that does not change in varying dc fields along this crystal direction.

The influence of the changes in the magnetic structure and the influence of superconductivity on the measured signal are clearly distinguishable in these ac measurements. Due to the hysteretic behavior in the superconducting state, an out-of-phase peak appears in the superconducting transition, its maximum indicating the temperature at which the sample is fully penetrated by the ac field. Figure 2 shows both, the in-phase and the out-of-phase signal for an ac measurement at 125 mT. One out-of-phase peak occurs, when superconductivity sets in at about 7.3 K, and the reentrant behavior is responsible for two other peaks at 4.9 and 5.4 K. The magnetic phase transitions, indicated by the dashed-dotted lines in Fig. 2, do not exhibit this feature, if they are not hysteretic. In fact, at least the transition T_N shows hysteretic be-

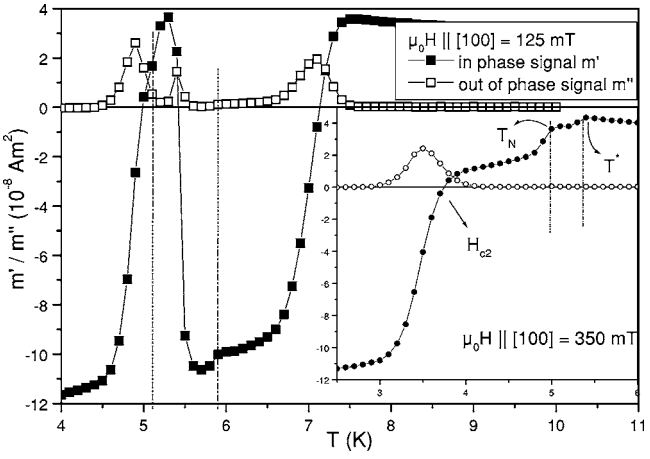

FIG. 2. In-phase and out-of-phase signal for an ac measurement at 125 mT. The peaks in the out-of-phase signal for the superconducting transitions are two orders of magnitude larger than the peaks related to hysteretic magnetic transitions, which are indicated by the vertical dash-dotted lines. The inset shows the result for 350 mT.

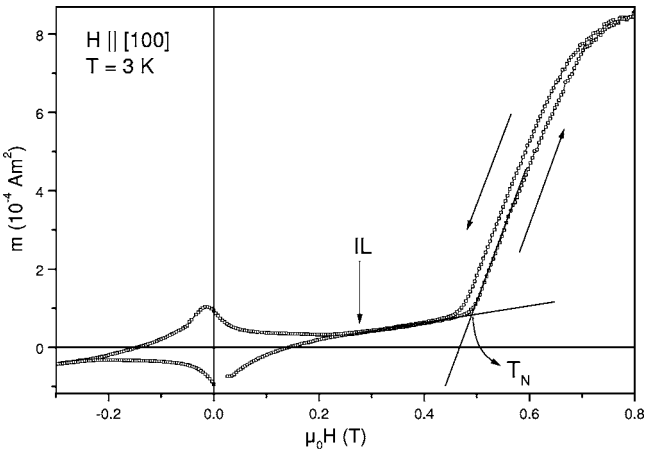

FIG. 3. Loop measurement at 3 K for the field applied along the [100] crystal direction. The irreversibility point and the evaluation criterion for the magnetic transition T_N are shown. The hysteretic behavior of T_N in increasing and decreasing fields is indicated by arrows.

havior, as will be discussed later, but the out-of-phase peak related to this transition can be hardly resolved on the scale of the peaks related to the superconducting transitions. A second example at a higher field of 350 mT demonstrates this observation more clearly for the transitions T_N and T^* (cf. the inset of Fig. 2).

The irreversibility points were taken from $m(T)$ as well as from $m(\mu_0 H)$-loop measurements in the SQUID and the VSM. The results of these different measurements fall within experimental accuracy. Figures 3 and 4 show examples for both types of results, respectively. The field dependent magnetic moments $m(\mu_0 H)$ reveal the irreversibility point *IL*, where the curves in increasing and decreasing external fields merge, whereas in the $m(T)$ measurements the merging points of zero-field-cooled (zfc) and field-cooled (fc) curves were evaluated (arrows in Fig. 4).

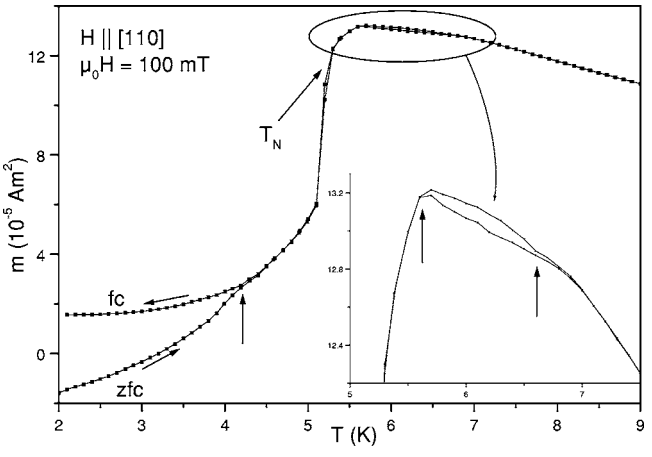

FIG. 4. Zero-field-cooled (zfc) and field-cooled (fc) curves of a $m(T)$ measurement at 100 mT for the field applied along the [110] crystal direction. The arrows indicate the irreversibility points and the magnetic transitions manifest themselves in a decrease of the magnetic moment between 5.1 and 5.6 K.

The magnetic transitions can also be seen in these measurements. Again $m(T)$ results and $m(\mu_0 H)$-loops can be compared. The loops show the magnetic transitions as changes in the slope of the magnetization curve, for the evaluation criterion see Fig. 3. Mainly the transition T_N, at 5.2 K in zero field, shows some hysteretic behavior in increasing and decreasing fields (cf. the arrows in Fig. 3 and also Ref. 4). In the $m(T)$ measurements, this transition manifests itself as a sharp decrease of the magnetic moment in all three crystal directions. Even for $H \| [001]$, where this transition should not be present, some indications are still observed due to a slighly imperfect sample orientation. However, the signal from the magnetically ordered structures is at least one order of magnitude smaller than that for field directions within the *ab* plane.

III. PHASE DIAGRAMS

T_c was determined to be 8.34 K, the width of the transition (10%–90%) was 0.2 K and the onset started at 8.5 K.

Figure 5 shows the phase diagram for magnetic fields applied parallel to the [100], the [110] and the [001] crystal directions, respectively (the lines are guides to the eye). A comparison of H_{c2} and the irreversibility line for these three crystal directions is shown in the inset of Fig. 5(c). The temperature dependence of H_{c2} is nonmonotonic and clearly shows the reentrant behavior. The occurrence of magnetic order heavily suppresses the superconducting parameters, such as $H_{c2}(T)$ and the irreversibility line *IL*. This is associated with increased pair breaking of the Cooper pairs due to metamagnetic ordering between ~5 and 6 K and the disappearance of this effect below the magnetic transition T_N into the antiferromagnetically ordered state.[3] The results for the magnetic transitions in the explored field and temperature range are in good agreement with previously published data (e.g., cf. Refs. 8 and 14). We wish to point out that the transition T_m in [100] direction does not shift with increasing field and, therefore, appears as a straight line in the phase diagram (cf. also Fig. 1), whereas it shifts to lower temperatures in [110] direction. This was reported in Refs. 9 and 14 and is confirmed by our results.

The magnetic transitions also manifest themselves in angular dependent measurements of the magnetic moment. Such measurements at fixed field and temperature were performed in a VSM, where the external field direction was rotated either within the *ab* plane or within the *ac* plane.

Figure 6 shows an example for a rotation in the *ac* plane at 3 K and 600 mT. For these parameters, the phase diagrams for $H \| [100]$ and $H \| [001]$ show that the sample is in a metamagnetically ordered state without superconductivity for $H \| [100]$ and that neither magnetic order nor superconductivity prevail for $H \| [001]$. Rotating the sample between these two directions leads to two different regimes that are separated by the magnetic phase transition B_N (see vertical dash-dotted lines in Fig. 6). The effective field value $\mu_0 H_0 \cos \varphi_0$ for the magnetic moments along the [100] crystal direction is identical within experimental accuracy with the field value of transition B_N at 3 K in the phase diagram for fields along the [100] direction (φ_0 denotes the angle

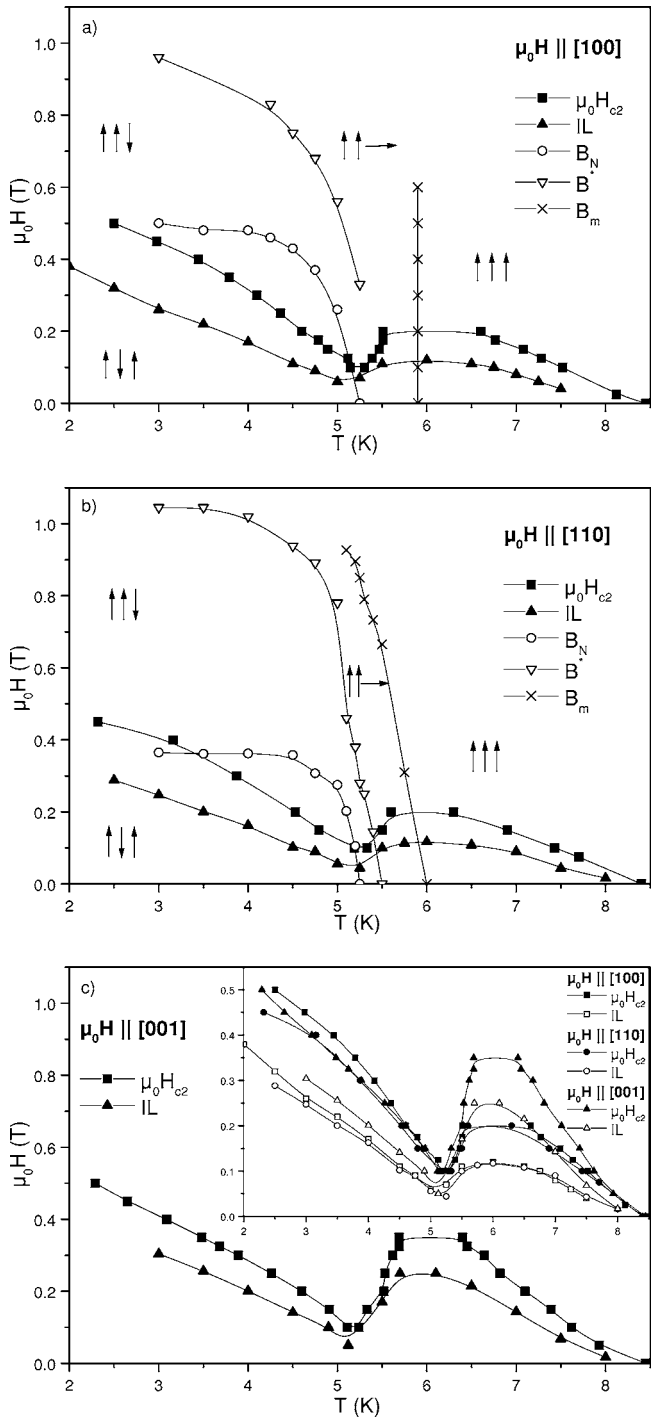

FIG. 5. Phase diagram for magnetic fields along the [100], the [110], and the [001] directions of the $HoNi_2B_2C$ single crystal showing the H_{c2} curve and the irreversibility line *IL*. The inset in (c) shows a comparison for all three crystal directions. For measurements in the *ab* plane, the magnetic transition lines are also shown and magnetic phases indicated by arrows.

between $\mu_0 H_0 \| [100]$ and the angular position, where the transition B_N occurs). In agreement with all other results, the magnetic moment for $H \| [001]$ is smaller by one order of magnitude than that for $H \| [100]$. As expected, the orthogonal moment is zero for field directions that are exactly parallel to the crystal axes.

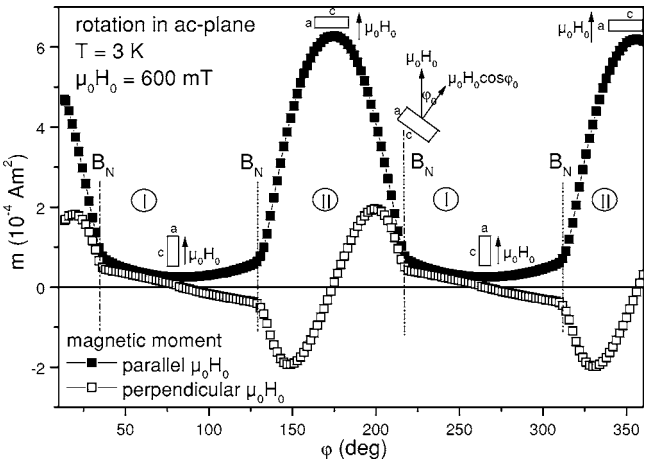

FIG. 6. Angle dependent magnetic moment parallel to (full squares) and perpendicular to the applied field (open circles) at 3 K and 600 mT. The magnetic phase transition T_N is indicated by four vertical dash-dotted lines. For angles in area I, neither superconductivity nor magnetic order prevail, whereas in area II, the sample is in a metamagnetically ordered state. The sample orientation is shown at these angular positions, where the field is directed along [100] and [001].

IV. CRITICAL CURRENTS

The irreversible magnetic moments of the magnetization loops below the irreversibility line were used to determine the critical current density J_c from the Bean model.[29] This can be done safely, because the loop measurements show symmetric irreversible magnetization curves and large remanent fields as demonstrated by the data for $H \| [001]$ shown in Fig. 7 as an example for all our results.

Figures 8 and 9 show the critical current densities for fields parallel to [100] and [001], respectively, the insets present their temperature dependence. For both field direc-

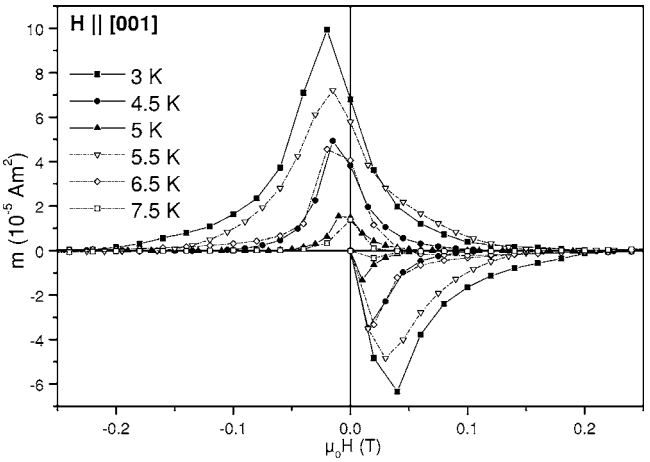

FIG. 7. Loop measurements for fields along [001] at different temperatures covering all regimes of magnetic order.

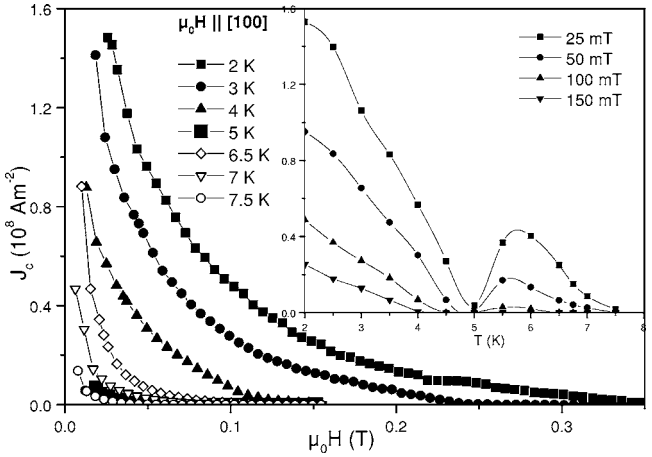

FIG. 8. Critical current densities for fields along [100] at different temperatures. A minimum is reached at 5 K. The inset shows the temperature dependence of J_c for four selected field values.

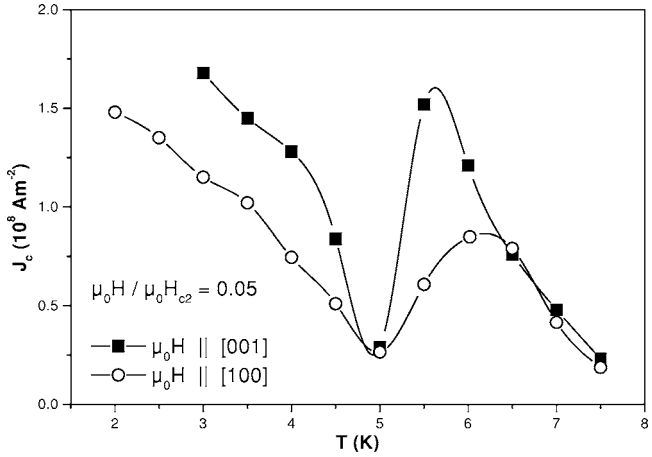

FIG. 10. Critical current densities as a function of temperature at the same reduced field of $H/H_{c2}=0.05$ for fields along [001] and [100].

tions, J_c has a minimum at about 5 K due to the magnetic phase transitions. At temperatures above 5 K, J_c increases again and reaches a maximum at 5.7 K, again for both crystal directions, but J_c at the peak is much larger for $H\|[001]$ (1.2×10^8 Am^{-2} at 25 mT) than for $H\|[100]$ (4.3×10^7 Am^{-2} at 25 mT).

These results establish a direct correlation between the pinning properties and the suppression of the superconducting state by the formation of metamagnetic order in the temperature range between 5 and 6 K, in agreement with the behavior of the irreversibility lines in the phase diagrams. Strong pinning only appears in those regions of the phase diagram, where superconductivity can fully develop and is not suppressed by the magnetic structures between T_N and T_m. The critical currents at 3 K and at low fields are of the order of 10^8 Am^{-2}.

In order to emphasize the rapid evolvement of flux pinning below T_c, the temperature dependence of J_c is plotted for two field orientations ([001] and [100]) in Fig. 10 for the same (low) reduced field. The steep increase of J_c initially scales for both orientations before dropping to almost zero at the magnetic transition temperature. The increase of J_c at low temperatures is less steep and does not scale, thus indicating different effects of pair breaking on J_c depending on the field orientation.

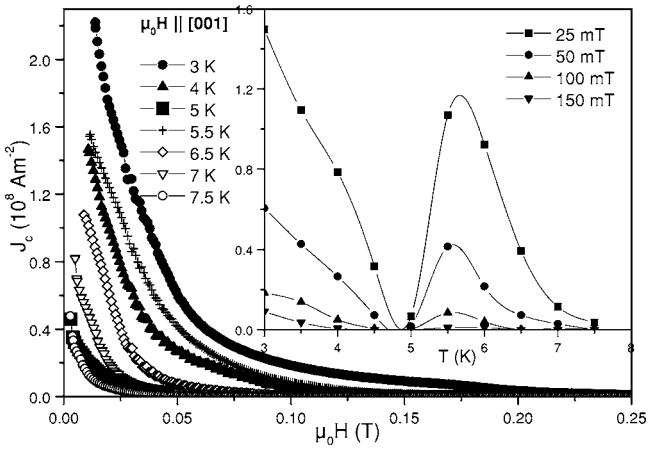

FIG. 9. Critical current densities for fields along [001] at different temperatures. The minimum is also reached at 5 K. The inset shows the temperature dependence of J_c at four selected fields.

These findings are in contrast to those of Ref. 24, where significant bulk pinning for $H\|[001]$ was found to appear only in the small temperature range, where H_{c2} is suppressed, and surface pinning was claimed to be dominant in all other regions of the phase diagram. The authors assumed bulk pinning to be due to some interaction of the flux lines with the metamagnetically ordered states. In contrast, consider the loops measured on our single crystal for $H\|[001]$ at temperatures, where the sample is in different magnetically ordered states (Fig. 7). Symmetric and qualitatively similar results are found at all temperatures, indicating bulk pinning over the whole temperature range. The shift of the maximum in the magnetization curve is consistent with the self field in positive and negative fields. This confirms (together with the symmetric shape of the curves) that the flux lines cannot leave the sample more easily in decreasing fields than penetrate it in increasing fields. Another important difference to the results of Ref. 24 is the large remanent magnetization observed at all temperatures. Contrary, the measurements presented in Ref. 24 showed only a small remanent magnetization and asymmetric curves in increasing and decreasing fields at those temperatures, where surface pinning appeared.

Some differences in the results might come from the smaller geometrical aspect ratio of our sample, since a higher aspect ratio favors surface pinning effects. In addition, comparing the phase diagram of Ref. 24 with that of our case for the [001] crystal direction, we note slightly different values of the upper critical field. This might indicate that our sample is less clean (smaller T_c, steeper H_{c2} curve), which could also lead to some defect clustering and, therefore, enhance bulk pinning, but such an effect can certainly not be invoked to explain a change from surface to bulk pinning.

Based on our experimental data, we believe that the results provide evidence for bulk pinning in the entire region of the phase diagram, where superconductivity occurs. To

interpret our results, we suggest the simplest and, therefore, most preferable explanation, i.e., that J_c in the temperature range from T_c to 6.5 K (Fig. 10), where the data for both crystal directions scale, would continue to raise at lower temperatures if magnetic ordering were absent. However, J_c is suppressed due to pair breaking by magnetic ordering.

V. SUMMARY

We have presented a thorough characterization of a $HoNi_2B_2C$ single crystal in the superconducting and the magnetically ordered state. The upper critical field was evaluated from ac measurements, the irreversibility points were identified in $m(\mu_0 H)$ as well as in $m(T)$ curves. The magnetic phase transitions for fields within the *ab* plane were mainly taken from $m(\mu_0 H)$ measurements.

The transition B_m in fields along the [110] direction exhibits a temperature dependence in agreement with Ref. 14. Angular dependent measurements of the magnetic moment at fixed field and temperature also reveal the magnetic transitions, confirming the above results.

Phase diagrams determined by magnetic measurements for fields applied along the [100], the [110], and the [001] crystal directions were presented. The upper critical fields for the [001] direction and for fields within the *ab* plane (mostly the [110] direction) agree qualitatively with published results determined by different experimental techniques. We report here on a complete assessment of the in-plane anisotropy of the upper critical field, which is found to be rather small (9% at 3 K) and pronounced only below T_N.

The critical current densities in $HoNi_2B_2C$ single crystals for fields along the [100] and [001] crystal directions were evaluated, they are of the order of 10^8 Am^{-2} at 3 K. The temperature dependence of J_c has a minimum at 5 K for both directions, reflecting the suppression of superconductivity by metamagnetic order prevailing between 5 and 6 K. Loop measurements further provide evidence for bulk pinning in this material in the entire temperature range of the phase diagram.

ACKNOWLEDGMENTS

The authors thank H. Hartmann for technical assistance. The authors would also like to thank D. Souptel from IFW Dresden for assisting with the preparation of the $HoNi_2B_2C$ single crystal. That part of work was supported by the Deutsche Forschungsgemeinschaft within the SFB 463 "Rare-Earth Intermetallics: Structure, Magnetism and Transport."

*Corresponding author. Electronic address: krutzler@ati.ac.at

[1] L. M. Dezaneti, Y. Y. Xue, Y. Y. Sun, K. Ross, and C. W. Chu, Physica C **334**, 123 (2000).
[2] K. H. Müller, G. Fuchs, S. L. Drechsler, and V. N. Narozhnyi, *Handbook of Magnetic Materials*, edited by K. H. Buschow (Elsevier Science, Amsterdam, 2002), Vol. 14, Chap. 3.
[3] A. I. Goldman, C. Stassis, P. C. Canfield, J. Zarestky, P. Dervenagas, B. K. Cho, D. C. Johnston, and B. Sternlieb, Phys. Rev. B **50**, R9668 (1994).
[4] T. E. Grigereit, J. W. Lynn, R. J. Cava, J. J. Krajewski, and W. F. Peck Jr., Physica C **248**, 382 (1995).
[5] J. W. Lynn, S. Skanthakumar, Q. Huang, S. K. Sinha, Z. Hossain, L. C. Gupta, R. Nagarajan, and C. Godart, Phys. Rev. B **55**, 6584 (1997).
[6] P. C. Canfield, S. L. Budko, B. K. Cho, A. Lacerda, D. Farrell, E. Johnston-Halperin, V. A. Kalatsky, and V. L. Pokrovsky, Phys. Rev. B **55**, 970 (1997).
[7] C. Detlefs, F. Bourdarot, P. Burlet, P. Dervenagas, S. L. Budko, and P. C. Canfield, Phys. Rev. B **61**, R14916 (2000).
[8] K. D. D. Rathnayaka, D. G. Naugle, B. K. Cho, and P. C. Canfield, Phys. Rev. B **53**, 5688 (1996).
[9] D. G. Naugle, K. D. D. Rathnayaka, A. K. Bhatnagar, A. C. Du Mar, A. Parasiris, J. M. Bell, P. C. Canfield, and B. K. Cho, Czech. J. Phys. **46**, Suppl. S6, 3263 (1996).
[10] A. J. Campbell, D. McK. Paul, and G. J. McIntyre, Phys. Rev. B **61**, 5872 (2000).
[11] V. A. Kalatsky and V. L. Pokrovsky, Phys. Rev. B **57**, 5485 (1998).
[12] A. Amici and P. Thalmeier, Phys. Rev. B **57**, 10684 (1998).
[13] A. Kreyssig, J. Freudenberger, C. Sierks, M. Loewenhaupt, K. H. Müller, A. Hoser, and N. Stuesser, Physica B **259–261**, 590 (1999).
[14] T. Park, M. B. Salamon, Eun Mi Choi, Heon Jung Kim, and Sung-Ik Lee, Phys. Rev. B **69**, 054505 (2004).
[15] T. A. Wagner, A. Dertinger, W. Ettig, A. Krause, H. Schmidt, and H. F. Braun, Physica C **323**, 71 (1999).
[16] A. Dertinger, R. E. Dinnebier, A. Kreyssig, P. W. Stephens, S. Pagola, M. Loewenhaupt, S. van Smaalen, and H. F. Braun, Phys. Rev. B **63**, 184518 (2001).
[17] C. V. Tomy, L. J. Chang, D. McK. Paul, N. H. Andersen, and M. Yethiraj, Physica B **213–214**, 139 (1995).
[18] J. W. Lynn, Q. Huang, A. Santoro, R. J. Cava, J. J. Krajewski, and W. F. Peck Jr., Phys. Rev. B **53**, 802 (1996).
[19] K. H. Müller, A. Kreyssig, A. Handstein, G. Fuchs, C. Ritter, and M. Loewenhaupt, J. Appl. Phys. **81**, 4240 (1997).
[20] U. Yaron, P. L. Gammel, A. P. Ramirez, D. A. Huse, D. J. Bishop, A. I. Goldman, C. Stassis, P. C. Canfield, K. Mortensen, and M. R. Eskildsen, Nature (London) **382**, 236 (1996).
[21] M. R. Eskildsen, P. L. Gammel, B. P. Barber, A. P. Ramirez, D. J. Bishop, N. H. Andersen, K. Mortensen, C. A. Bolle, C. M. Lieber, and P. C. Canfield, Phys. Rev. Lett. **79**, 487 (1997).
[22] D. McK. Paul, C. V. Tomy, C. M. Aegerter, R. Cubitt, S. H. Lloyd, E. M. Forgan, S. L. Lee, and M. Yethiraj, Phys. Rev. Lett. **80**, 1517 (1998).
[23] M. R. Eskildsen, K. Harada, P. L. Gammel, A. B. Abrahamsen, N. H. Andersen, G. Ernst, A. P. Ramirez, D. J. Bishop, K. Mortensen, D. G. Naugle, K. D. D. Rathnayaka, and P. C. Canfield, Nature (London) **393**, 242 (1998).
[24] C. D. Dewhurst, R. A. Doyle, E. Zeldov, and D. McK. Paul, Phys. Rev. Lett. **82**, 827 (1999).
[25] C. D. Dewhurst, S. S. James, R. A. Doyle, Y. Paltiel, H. Shtrikman, E. Zeldov, and D. McK. Paul, Phys. Rev. B **63**, 060501(R)

(2001).
[26] S. S. James, C. D. Dewhurst, S. B. Field, D. McK. Paul, Y. Paltiel, H. Shtrikman, E. Zeldov, and A. M. Campbell, Phys. Rev. B **64**, 092512 (2001).
[27] D. Souptel, G. Behr, A. Kreyssig, and W. Löser, J. Cryst. Growth **276**, 652 (2005).
[28] D. Souptel, G. Behr, W. Löser, K. Nenkov, and G. Fuchs, J. Cryst. Growth **275**, e91 (2005).
[29] C. P. Bean, Phys. Rev. Lett. **8**, 250 (1962).